

# Synthesis, Crystal Structure and Electrical Properties of Two New Palladium Complexes of Selenium and Sulfur Ligands: $[\text{NMe}_4][\text{Pd}(\text{C}_3\text{S}_3\text{Se}_2)_2]_2$ and $[\text{PMe}_4][\text{Pd}(\text{C}_3\text{S}_5)_2]_2$ <sup>†</sup>

Christophe Faulmann,<sup>a</sup> Jean-Pierre Legros,<sup>a</sup> Patrick Cassoux,<sup>\*,a</sup> Joost Cornelissen,<sup>b</sup> Luc Brossard,<sup>c</sup> Makoto Inokuchi,<sup>d</sup> Hiroyuki Tajima<sup>d</sup> and Madoka Tokumoto<sup>e</sup>

<sup>a</sup> *Laboratoire de Chimie de Coordination du CNRS, 205 route de Narbonne, 31077 Toulouse Cedex, France*

<sup>b</sup> *Department of Chemistry, Gorlaeus Laboratories, Leiden University, P.O. Box 9502, 2300 RA Leiden, The Netherlands*

<sup>c</sup> *Laboratoire de Physique des Solides (UA 074, CNRS) INSA, Complexe Scientifique de Rangueil, 31077 Toulouse Cedex, France*

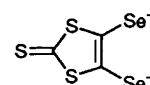
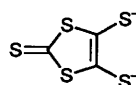
<sup>d</sup> *Department of Chemistry, Faculty of Science, The University of Tokyo, Hongo, Bunkyo-ku, 113 Tokyo, Japan*

<sup>e</sup> *Electrotechnical Laboratory, 1-1-4 Umenozo, Tsukuba, Ibaraki 305, Japan*

The compounds  $[\text{NMe}_4][\text{Pd}(\text{C}_3\text{S}_3\text{Se}_2)_2]_2$  and  $[\text{PMe}_4][\text{Pd}(\text{C}_3\text{S}_5)_2]_2$  [ $\text{C}_3\text{S}_3\text{Se}_2 = 4,5$ -bis(hydroseleno)-1,3-dithiole-2-thionate;  $\text{C}_3\text{S}_5 = 4,5$ -dimercapto-1,3-dithiole-2-thionate] have been prepared by electrochemical oxidation of  $[\text{NBu}_4][\text{Pd}(\text{C}_3\text{S}_3\text{Se}_2)_2]$  and  $[\text{NBu}_4][\text{Pd}(\text{C}_3\text{S}_5)_2]$  in the presence of a large excess of  $\text{NMe}_4\text{PF}_6$  and  $\text{PMe}_4\text{I}$ , respectively. Their structures have been determined by X-ray crystallographic methods. Both compounds, with space group  $C2/c$ , are isostructural to the superconducting phase  $\beta$ - $[\text{NMe}_4][\text{Pd}(\text{C}_3\text{S}_5)_2]_2$ . The  $\text{PdL}_2$  ( $\text{L} = \text{C}_3\text{S}_3\text{Se}_2$  or  $\text{C}_3\text{S}_5$ ) entities are paired, forming  $[(\text{PdL}_2)_2]$  dimers with a Pd–Pd bond length of 3.174 and 3.177 Å, respectively. The structure consists of  $[(\text{PdL}_2)_2]$  dimer layers in the (001) plane separated from each other by sheets of cations. The dimers are stacked along  $[110]$  and  $[1\bar{1}0]$ . Both compounds show similar electrical properties: the room-temperature conductivities are  $\approx 50$  and  $\approx 20 \text{ S cm}^{-1}$ , respectively; at high temperature the conductivity is weakly temperature dependent, but abruptly decreases at low temperatures; the conductivity increases when applying pressure. A broad dispersion of optical excitations was observed in the reflectance spectra of  $[\text{NMe}_4][\text{Pd}(\text{C}_3\text{S}_3\text{Se}_2)_2]_2$ , indicating an overlap of the highest occupied (HOMO) and lowest unoccupied molecular orbital (LUMO) bands and a HOMO-type conduction band.

To date more than seventy compounds derived from the metal complexes of  $\text{C}_3\text{S}_5^{2-}$  (4,5-dimercapto-1,3-dithiole-2-thionate) have been prepared and studied.<sup>1</sup> Among these a number of molecular metals and six phases superconducting under pressure have been characterized.<sup>2–5</sup> Recently, two of us have observed superconductivity at ambient pressure at 1.3 K in  $\alpha$ - $[\text{edt-ttf}][\text{Ni}(\text{C}_3\text{S}_5)_2]_2$  ( $\text{edt-ttf} = \text{C}_8\text{H}_6\text{S}_6 = \text{ethylenedithio-tetrathiafulvalene}$ ).<sup>6</sup> In addition of superconductivity, these systems exhibit interesting properties, such as a pressure dependence of the critical temperature,<sup>7</sup> the presence of charge-density wave states,<sup>8</sup> which, in some cases, do not induce a metal-to-insulator transition,<sup>9</sup> these properties being related to a unique multi-sheets band structure.<sup>10</sup>

For the  $\beta$ - $[\text{NMe}_4][\text{Pd}(\text{C}_3\text{S}_5)_2]_2$  phase as well as for the other superconducting members of the  $\text{M}(\text{C}_3\text{S}_5)_2$  series containing closed-shell cation the space group is  $C2/c$ ,<sup>2–4</sup> except for  $[\text{NMe}_2\text{Et}_2][\text{Pd}(\text{C}_3\text{S}_5)_2]_2$  for which the space group is  $P\bar{1}$ .<sup>5</sup> Is this structural feature at the origin of superconductivity, or is it just a coincidence? It should be also noted in all of the  $\text{M}(\text{C}_3\text{S}_5)_2$  superconductors with a closed-shell cation<sup>3–5</sup> the cation has a tetrahedral ( $\text{NMe}_4$ ) or pseudo-tetrahedral ( $\text{NEt}_2\text{Me}_2$ ) symmetry. Moreover, previous studies on  $\text{M}(\text{C}_3\text{S}_5)_2$  systems have shown that even small chemical modifications from one



compound to another may result in dramatic changes in their properties, for the better or for the worse. For example, the methyl derivative  $[\text{NMe}_4][\text{Ni}(\text{C}_3\text{S}_5)_2]_2$  is superconducting,<sup>3</sup> whereas the ethyl derivative  $[\text{NEt}_4][\text{Ni}(\text{C}_3\text{S}_5)_2]_2$  is not.<sup>11</sup>

We report in this paper the synthesis, crystal structure and electrical properties of two new palladium complexes, isostructural to  $\beta$ - $[\text{NMe}_4][\text{Pd}(\text{C}_3\text{S}_5)_2]_2$ , obtained by formally substituting in  $\beta$ - $[\text{NMe}_4][\text{Pd}(\text{C}_3\text{S}_5)_2]_2$ , either the selenium-based ligand  $\text{C}_3\text{S}_3\text{Se}_2^{2-}$  [4,5-bis(hydroseleno)-1,3-dithiole-2-thionate] for the  $\text{C}_3\text{S}_5^{2-}$  ligand, which gives  $[\text{NMe}_4][\text{Pd}(\text{C}_3\text{S}_3\text{Se}_2)_2]_2$ , or the tetramethylphosphonium for the tetramethylammonium cation, which gives  $[\text{PMe}_4][\text{Pd}(\text{C}_3\text{S}_5)_2]_2$ . A preliminary report has appeared on  $[\text{NMe}_4][\text{Pd}(\text{C}_3\text{S}_3\text{Se}_2)_2]_2$ .<sup>12</sup>

## Experimental

**Synthesis and Crystal Growth.**—The complexes  $[\text{NBu}_4][\text{Pd}(\text{C}_3\text{S}_3\text{Se}_2)_2]$  and  $[\text{NBu}_4][\text{Pd}(\text{C}_3\text{S}_5)_2]$  were prepared as in ref. 13 and 14, respectively. Shiny black platelet-like crystals of  $[\text{NMe}_4][\text{Pd}(\text{C}_3\text{S}_3\text{Se}_2)_2]_2$  were obtained following a 'large excess method' similar to that previously described for several closed-shell cation complexes of  $\text{C}_3\text{S}_5^{2-}$ ,<sup>15</sup> by galvanostatic (5  $\mu\text{A}$ ) electrochemical oxidation on a platinum anode of an

<sup>†</sup> *Supplementary data available:* see Instructions for Authors, *J. Chem. Soc., Dalton Trans.*, 1994, Issue 1, pp. xxiii–xxviii.

*Non-SI unit employed:* bar =  $10^5$  Pa.

acetonitrile solution of  $[\text{NBu}_4][\text{Pd}(\text{C}_3\text{S}_3\text{Se}_2)_2]$  ( $1.7 \times 10^{-3}$  mol  $\text{dm}^{-3}$ ) containing a large excess ( $1.7 \times 10^{-2}$  mol  $\text{dm}^{-3}$ ) of  $\text{NMe}_4\text{PF}_6$ . Black acicular crystals of  $[\text{PMe}_4][\text{Pd}(\text{C}_3\text{S}_3\text{Se}_2)_2]$  were obtained following a similar procedure, by galvanostatic (1  $\mu\text{A}$ ) electrochemical oxidation of an acetonitrile solution of  $[\text{NBu}_4][\text{Pd}(\text{C}_3\text{S}_3\text{Se}_2)_2]$  ( $7 \times 10^{-4}$  mol  $\text{dm}^{-3}$ ) containing a large excess ( $2 \times 10^{-2}$  mol  $\text{dm}^{-3}$ ) of  $\text{PMe}_4\text{I}$ .

**Crystallography.**<sup>16</sup>—**Crystal data.**  $\text{C}_{16}\text{H}_{12}\text{NPd}_2\text{S}_{12}\text{Se}_8$ ,  $M = 1447.53$ , monoclinic, space group  $C2/c$ ,  $a = 14.675(4)$ ,  $b = 6.547(1)$ ,  $c = 35.400(8)$  Å,  $\beta = 91.58(2)^\circ$ ,  $U = 3400(1)$  Å<sup>3</sup> (by least-squares refinement on diffractometer angles for 25 automatically centred reflections,  $\lambda = 0.71069$  Å),  $Z = 4$ ,  $D_c = 2.83$  g  $\text{cm}^{-3}$ ,  $F(000) = 2684$ . Shiny black platelets. Crystal dimensions  $0.3 \times 0.3 \times 0.1$  mm,  $\mu(\text{Mo-K}\alpha) = 102.5$   $\text{cm}^{-1}$ .

$\text{C}_{16}\text{H}_{12}\text{PPd}_2\text{S}_{20}$ ,  $M = 1089.33$ , monoclinic, space group  $C2/c$ ,  $a = 14.373(2)$ ,  $b = 6.354(1)$ ,  $c = 36.481(5)$  Å,  $\beta = 98.13(1)^\circ$ ,  $U = 3298(1)$  Å<sup>3</sup> (by least-squares refinement as above),  $Z = 4$ ,  $D_c = 2.19$  g  $\text{cm}^{-3}$ ,  $F(000) = 2140$ . Shiny black needles. Crystal dimensions  $0.5 \times 0.2 \times 0.15$  mm,  $\mu(\text{Mo-K}\alpha) = 23.6$   $\text{cm}^{-1}$ .

**Data collection and processing.** In both cases the intensity of three reflections was monitored throughout the data collection and no significant decay was observed. For  $[\text{NMe}_4][\text{Pd}(\text{C}_3\text{S}_3\text{Se}_2)_2]$ , a CAD4 diffractometer,  $\omega$ - $2\theta$  mode with  $\omega$  scan width =  $0.75 + 0.35 \tan\theta$ , variable  $\omega$  scan speed, and graphite-monochromated Mo-K $\alpha$  radiation were employed. 2161 Reflections measured ( $1.5 \leq \theta \leq 22^\circ$ ,  $+h$ ,  $+k$ ,  $\pm l$ ), giving 1191 independent with  $I > 2\sigma(I)$ . Similarly for  $[\text{PMe}_4][\text{Pd}(\text{C}_3\text{S}_3\text{Se}_2)_2]$ , except  $\omega$  scan width =  $0.80 + 0.35 \tan\theta$ ; 4774 reflections measured ( $2 \leq \theta < 30^\circ$ ,  $+h$ ,  $+k$ ,  $\pm l$ ), giving 2632 independent with  $I > 3\sigma(I)$ .

For both compounds, an empirical absorption correction based on  $\psi$  scans was applied to the data set. Transmission coefficients: 0.6179–0.9988 for  $[\text{NMe}_4][\text{Pd}(\text{C}_3\text{S}_3\text{Se}_2)_2]$  and 0.9107–0.9999 for  $[\text{PMe}_4][\text{Pd}(\text{C}_3\text{S}_3\text{Se}_2)_2]$ .

**Structure analysis and refinement.** Direct methods (Pd atoms) followed by normal heavy-atom procedures. Full-matrix least-squares refinement with all non-hydrogen atoms anisotropic {except the six carbon atoms of the  $\text{Pd}(\text{C}_3\text{S}_3\text{Se}_2)_2$  unit in  $[\text{NMe}_4][\text{Pd}(\text{C}_3\text{S}_3\text{Se}_2)_2]$ } and hydrogen atoms in calculated positions with  $B = 1.3B_{\text{iso}}(\text{C atom})$  Å<sup>2</sup>. Final  $R$  and  $R'$  were 0.034 and 0.068 for  $[\text{NMe}_4][\text{Pd}(\text{C}_3\text{S}_3\text{Se}_2)_2]$ , [ $w^{-1} = \sigma^2(F) + 0.0009F^2$ ], and 0.037 and 0.046 for  $[\text{PMe}_4][\text{Pd}(\text{C}_3\text{S}_3\text{Se}_2)_2]$  [ $w^{-1} = \sigma^2(F) + 0.0004F^2$ ]. The maximum shift/e.s.d. in the final refinements was 0.13 and 0.20 for  $[\text{NMe}_4][\text{Pd}(\text{C}_3\text{S}_3\text{Se}_2)_2]$  and  $[\text{PMe}_4][\text{Pd}(\text{C}_3\text{S}_3\text{Se}_2)_2]$ , respectively. The maximum and minimum residual densities in the final Fourier difference maps were 0.49 and  $-0.56$  and 0.39 and  $-0.67$  e Å<sup>-3</sup> respectively. All calculations were performed on a VAX 11/730 computer. Programs used and sources of scattering factor data are given in ref. 16.

Atomic coordinates for the non-hydrogen atoms are listed in Tables 1 and 2, and bond lengths and angles in Tables 3 and 4, for  $[\text{NMe}_4][\text{Pd}(\text{C}_3\text{S}_3\text{Se}_2)_2]$  and  $[\text{PMe}_4][\text{Pd}(\text{C}_3\text{S}_3\text{Se}_2)_2]$ , respectively. The atomic numbering schemes are shown in Figs. 1 and 2.

Additional material available from the Cambridge Crystallographic Data Centre comprises for both compounds the H-atom coordinates, thermal parameters and remaining bond lengths and angles.

**Conductivity Measurements.**—The temperature dependence of the resistance of  $[\text{PMe}_4][\text{Pd}(\text{C}_3\text{S}_3\text{Se}_2)_2]$  crystals was measured along their long axis ( $b$ ). Ambient-pressure conductivity measurements were performed on three needle-shaped crystal samples using previously described techniques.<sup>17</sup> Conductivity measurements under pressure were performed on two crystal samples: the first was a long and thin elongated rod with a rectangular cross-section, and the second was a belly-shaped needle; the results were identical for both samples. A classical

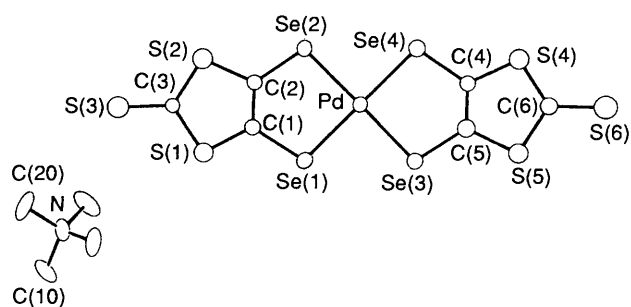


Fig. 1 The atomic numbering scheme of  $[\text{NMe}_4][\text{Pd}(\text{C}_3\text{S}_3\text{Se}_2)_2]$

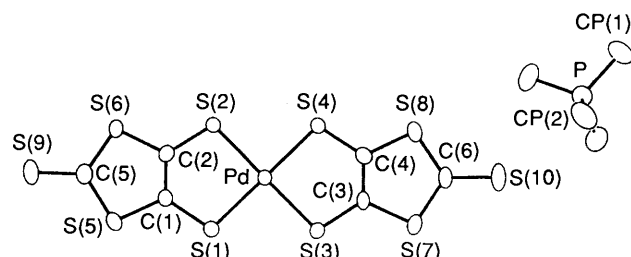


Fig. 2 The atomic numbering scheme of  $[\text{PMe}_4][\text{Pd}(\text{C}_3\text{S}_3\text{Se}_2)_2]$

lock-in technique was used to detect the in- and out-of-phase voltages obtained when feeding the samples with a low-frequency (6.66 Hz) alternating current of 2  $\mu\text{A}$ . The samples were connected to the measuring line through annealed gold wires (17  $\mu\text{m}$  diameter) which were fixed with silver paint to four evaporated gold contacts. The contact resistances at the electrodes were less than 10  $\Omega$  at room temperature. These wires were soldered to electrical feedthroughs mounted inside an obturator which was plugged into a Cu-Be pressure bomb filled with a mixture of lubricating oil and petrol. The pressure was monitored *via* recording the resistance of a highly doped InSb manometer, the metallic character of which is independent of the pressure below 22 kbar.

The temperature dependence of the resistance of three  $[\text{NMe}_4][\text{Pd}(\text{C}_3\text{S}_3\text{Se}_2)_2]$  samples was measured along the long axis of the platelets ( $b$ ) with a d.c. current of 10  $\mu\text{A}$ . The contact resistances at the electrode were less than 150  $\Omega$  at room temperature. Samples were pressurized by use of a clamp-type cell with an oil (Daphne no. 7373, Idemitsu Co.) as pressure medium. The pressure in the cell was measured from the resistance change of a manganin wire at room temperature.

**Reflectance Measurements.**—The reflectance spectrum of  $[\text{NMe}_4][\text{Pd}(\text{C}_3\text{S}_3\text{Se}_2)_2]$  was measured for the polarization parallel to the  $a$  and  $b$  axes, using previously described apparatus and techniques.<sup>18</sup>

## Results and Discussion

**Crystal Structure of  $[\text{NMe}_4][\text{Pd}(\text{C}_3\text{S}_3\text{Se}_2)_2]$ .**—The unit cell (Fig. 3) contains eight  $\text{Pd}(\text{C}_3\text{S}_3\text{Se}_2)_2$  entities and four  $\text{NMe}_4$  cations. The Pd- $\text{Se}$  bonds have a mean length of  $\approx 2.4$  Å, *i.e.* slightly longer than the mean Pd-S bond length ( $\approx 2.3$  Å) in isostructural  $\beta$ - $[\text{NMe}_4][\text{Pd}(\text{C}_3\text{S}_5)_2]$ .<sup>3,4</sup> The  $\text{Pd}(\text{C}_3\text{S}_3\text{Se}_2)_2$  entities are paired (Fig. 4), forming  $[\text{Pd}(\text{C}_3\text{S}_3\text{Se}_2)_2]_2$  dimers with a Pd-Pd bond length of 3.174 Å, similar to, but slightly longer than, those found in the isostructural  $\text{Pd}(\text{C}_3\text{S}_5)_2$  compounds: 3.116 Å in  $\beta$ - $[\text{NMe}_4][\text{Pd}(\text{C}_3\text{S}_5)_2]$ ,<sup>3,4</sup> 3.167 Å in  $[\text{AsMe}_4][\text{Pd}(\text{C}_3\text{S}_5)_2]$ ,<sup>3</sup> and 3.154 Å in  $\text{Cs}[\text{Pd}(\text{C}_3\text{S}_5)_2]$ .<sup>19</sup> The strong Pd-Pd interaction, and the ensuing  $\text{S} \cdots \text{S}$  repulsions, are evidenced by the perfectly eclipsed overlap of two  $\text{Pd}(\text{C}_3\text{S}_3\text{Se}_2)_2$  entities within a dimer (Fig. 5), and an out-of-plane displacement of the Pd atom from the  $\text{Se}_4$  plane (0.102 Å) significantly larger than the corresponding distance (0.07 Å) in

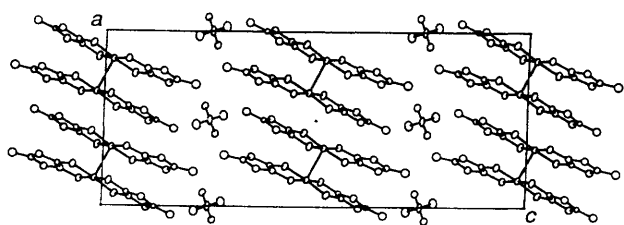


Fig. 3 The unit-cell contents of  $[\text{NMe}_4][\text{Pd}(\text{C}_3\text{S}_3\text{Se}_2)_2]_2$

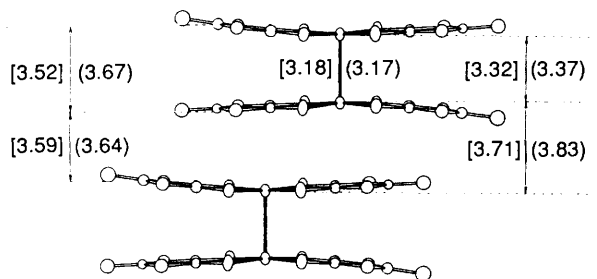


Fig. 4 Side view of two stacked  $[\text{PdL}_2]_2$  dimers. Numerical values ( $\text{\AA}$ ) between parentheses and square brackets refer to  $L = \text{C}_3\text{S}_3\text{Se}_2$  and  $\text{C}_3\text{S}_3$  respectively. The Pd–Pd and interplanar distances are given for (---) the  $\text{Se}_4$  or  $\text{S}_4$  co-ordination planes, and (---) the molecular mean planes

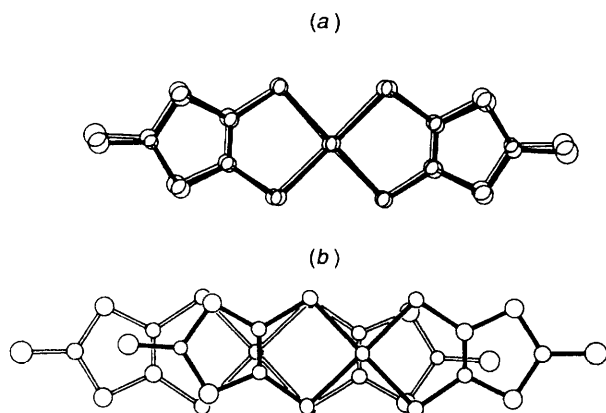


Fig. 5 Modes of overlap in  $[\text{NMe}_4][\text{Pd}(\text{C}_3\text{S}_3\text{Se}_2)_2]_2$  and  $[\text{PdMe}_4][\text{Pd}(\text{C}_3\text{S}_5)_2]_2$ : (a) intradimer, (b) interdimer

$\beta$ - $[\text{NMe}_4][\text{Pd}(\text{C}_3\text{S}_5)_2]_2$ .<sup>3,4</sup> It is interesting that in the present case the dimerization occurs *via* a Pd–Pd bond, whereas in the  $\alpha$ - and  $\beta$ - $[\text{NBu}_4][\text{Ni}(\text{C}_3\text{S}_3\text{Se}_2)_2]_2$  nickel phases<sup>13</sup> dimerization occurs *via* a Ni–Se bond between the nickel atom and a selenium atom of a neighbouring  $\text{Ni}(\text{C}_3\text{S}_3\text{Se}_2)_2$  entity.

The structure consists of  $[\text{Pd}(\text{C}_3\text{S}_3\text{Se}_2)_2]_2$  dimer layers in the (001) plane separated from each other by sheets of ordered  $\text{NMe}_4$  cations. The dimers are stacked along  $[110]$  and  $[1\bar{1}0]$ , a mode also observed in  $[\text{NMe}_4][\text{Ni}(\text{C}_3\text{S}_5)_2]_2$ .<sup>3</sup> Compared to  $\beta$ - $[\text{NMe}_4][\text{Pd}(\text{C}_3\text{S}_5)_2]_2$ , the anions in  $[\text{NMe}_4][\text{Pd}(\text{C}_3\text{S}_3\text{Se}_2)_2]_2$  seem to be just slightly less dimerized, as reflected by the longer Pd...Pd bond length (Fig. 4) and the somewhat smaller difference in the alternating interplanar spacings of the  $\text{S}_4$  or  $\text{Se}_4$  environment of the Pd atom (3.37, 3.83  $\text{\AA}$ , compared to 3.28, 3.82  $\text{\AA}$ ). Thus, substituting the sulfur for the larger selenium atoms has a small effect on the dimerization.

As in most  $\text{Pd}(\text{C}_3\text{S}_5)_2$  compounds,<sup>3,4,19</sup> the  $\text{Pd}(\text{C}_3\text{S}_3\text{Se}_2)_2$  anions along the stacks are perfectly eclipsed within a dimer, but the interdimer shear results in an essentially longitudinal offset (Fig. 5). A number of short (less than sum of the van der Waals radii) intermolecular chalcogen–chalcogen distances are present within the dimers, and between neighbouring stacks, as usually observed in  $\text{M}(\text{C}_3\text{S}_5)_2$  compounds,<sup>1</sup> but additional

Table 1 Fractional atomic coordinates for  $[\text{NMe}_4][\text{Pd}(\text{C}_3\text{S}_3\text{Se}_2)_2]_2$

Atom	x	y	z
Pd	0.158 7(1)	0.180 0(3)	0.519 20(4)
Se(1)	0.070 5(2)	0.352 5(3)	0.470 76(6)
Se(2)	0.146 7(2)	−0.137 0(3)	0.484 70(6)
Se(3)	0.155 4(1)	0.491 8(3)	0.555 20(6)
Se(4)	0.236 8(2)	0.004 4(3)	0.570 62(6)
S(1)	−0.003 3(4)	0.188 1(9)	0.394 4(1)
S(2)	0.052 9(4)	−0.224 4(9)	0.406 0(1)
S(3)	−0.050 5(4)	−0.120(1)	0.335 9(2)
S(4)	0.290 0(4)	0.167(1)	0.650 3(1)
S(5)	0.222 1(4)	0.573 4(9)	0.638 2(2)
S(6)	0.297 6(4)	0.466(1)	0.713 9(2)
C(1)	0.053(1)	0.140(3)	0.435 0(5)
C(2)	0.081(1)	−0.055(3)	0.441 8(5)
C(3)	−0.003(1)	−0.058(3)	0.376 8(5)
C(4)	0.242(1)	0.214(3)	0.606 4(5)
C(5)	0.210(1)	0.407(3)	0.600 0(6)
C(6)	0.272(1)	0.403(3)	0.669 0(5)
N	0.000	0.465(4)	0.250
C(10)	−0.080(1)	0.599(4)	0.237 8(6)
C(20)	0.026(2)	0.340(4)	0.217 4(6)

Table 2 Fractional atomic coordinates for  $[\text{PMe}_4][\text{Pd}(\text{C}_3\text{S}_5)_2]_2$

Atom	x	y	z
Pd	0.350 79(3)	0.327 09(7)	0.018 69(1)
S(1)	0.419 0(1)	0.162 6(3)	−0.027 11(4)
S(2)	0.345 7(1)	0.635 4(2)	−0.014 09(4)
S(3)	0.364 8(1)	0.023 4(3)	0.053 54(4)
S(4)	0.292 4(1)	0.501 2(3)	0.065 71(4)
S(5)	0.466 2(1)	0.319 7(3)	−0.099 64(4)
S(6)	0.404 1(1)	0.742 8(3)	−0.087 18(4)
S(7)	0.326 6(1)	−0.059 6(3)	0.131 25(4)
S(8)	0.263 8(1)	0.364 0(3)	0.141 64(4)
S(9)	0.471 5(1)	0.646 4(3)	−0.157 95(5)
S(10)	0.268 8(2)	0.061 5(4)	0.203 72(5)
P	0.000	0.216 7(5)	0.250
C(1)	0.422 3(4)	0.362(1)	−0.058 0(2)
C(2)	0.392 0(4)	0.563 4(9)	−0.052 1(2)
C(3)	0.327 4(4)	0.107(1)	0.093 1(2)
C(4)	0.296 7(4)	0.311(1)	0.098 8(2)
C(5)	0.448 2(4)	0.573(1)	−0.117 0(2)
C(6)	0.285 1(5)	0.119(1)	0.160 9(2)
CP(1)	−0.032 7(6)	0.380(1)	0.286 0(2)
CP(2)	−0.097 7(6)	0.051(1)	0.232 9(2)

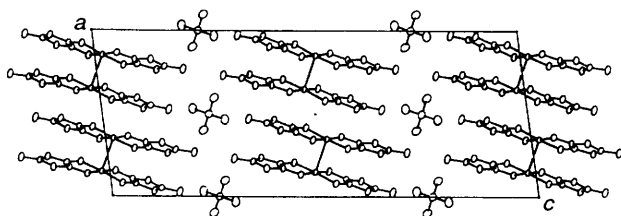
short chalcogen–chalcogen distances are also observed between stacked dimers (Supplementary material). The more spatially extended orbitals of selenium compared to sulfur increases the number of such interactions. However, Hückel-type calculations<sup>20</sup> show that, as in  $\beta$ - $[\text{NMe}_4][\text{Pd}(\text{C}_3\text{S}_5)_2]_2$ ,<sup>4</sup> the largest intermolecular orbital overlap is found within the dimers. In spite of the larger number of short intermolecular chalcogen–chalcogen distances within and between the stacks in  $[\text{NMe}_4][\text{Pd}(\text{C}_3\text{S}_3\text{Se}_2)_2]_2$ , only one transverse overlap integral is relatively large ( $\approx 1/5$  of the value within the dimer). As a result  $[\text{NMe}_4][\text{Pd}(\text{C}_3\text{S}_3\text{Se}_2)_2]_2$  seems to possess a slightly more two-dimensional character than the corresponding  $\beta$ - $[\text{NMe}_4][\text{Pd}(\text{C}_3\text{S}_5)_2]_2$  analogue.

**Crystal Structure of  $[\text{PMe}_4][\text{Pd}(\text{C}_3\text{S}_5)_2]_2$ .**—This compound is isostructural to  $[\text{NMe}_4][\text{Pd}(\text{C}_3\text{S}_3\text{Se}_2)_2]_2$ , and therefore to superconducting  $\beta$ - $[\text{NMe}_4][\text{Pd}(\text{C}_3\text{S}_5)_2]_2$ ,<sup>3,4</sup> and presents the same basic structural features. The unit cell (Fig. 6) contains eight  $\text{Pd}(\text{C}_3\text{S}_5)_2$  entities and four  $\text{PMe}_4$  cations. The Pd–S bond lengths (mean 2.298  $\text{\AA}$ ) and S–Pd–S angles (mean 89.94°) are similar to those observed in  $\beta$ - $[\text{NMe}_4][\text{Pd}(\text{C}_3\text{S}_5)_2]_2$  (2.295  $\text{\AA}$ , 89.95°)<sup>3,4</sup> and in  $[\text{AsMe}_4][\text{Pd}(\text{C}_3\text{S}_5)_2]_2$  (2.295  $\text{\AA}$ , 90.05°).<sup>4</sup> The  $\text{Pd}(\text{C}_3\text{S}_5)_2$  entities are paired (Fig. 4), forming  $[\{\text{Pd}(\text{C}_3\text{S}_5)_2\}_2]$

**Table 3** Bond lengths (Å) and angles (°) for  $[\text{NMe}_4][\text{Pd}(\text{C}_3\text{S}_3\text{Se}_2)_2]_2$ 

Pd–Pd <sup>d</sup>	3.174(3)	S(3)–C(3)	1.64(2)
Pd–Se(1)	2.401(3)	S(4)–C(4)	1.72(2)
Pd–Se(2)	2.411(3)	S(4)–C(6)	1.70(2)
Pd–Se(3)	2.408(3)	S(5)–C(5)	1.74(2)
Pd–Se(4)	2.416(3)	S(5)–C(6)	1.71(2)
Se(1)–C(1)	1.90(2)	S(6)–C(6)	1.68(2)
Se(2)–C(2)	1.85(2)	C(1)–C(2)	1.36(3)
Se(3)–C(5)	1.84(2)	C(4)–C(5)	1.36(3)
Se(4)–C(4)	1.87(2)	N–C(10)	1.52(3)
S(1)–C(1)	1.70(2)	N–C(10 <sup>II</sup> )	1.52(3)
S(1)–C(3)	1.73(2)	N–C(20)	1.47(3)
S(2)–C(2)	1.73(2)	N–C(20 <sup>II</sup> )	1.47(3)
S(2)–C(3)	1.70(2)		
Pd <sup>d</sup> –Pd–Se(1)	90.17(9)	Se(2)–C(2)–C(1)	125(2)
Pd <sup>d</sup> –Pd–Se(2)	94.72(9)	S(2)–C(2)–C(1)	114(2)
Pd <sup>d</sup> –Pd–Se(3)	90.64(9)	S(1)–C(3)–S(2)	114(1)
Pd <sup>d</sup> –Pd–Se(4)	94.07(9)	S(1)–C(3)–S(3)	122(1)
Se(1)–Pd–Se(2)	90.74(9)	S(2)–C(3)–S(3)	124(1)
Se(1)–Pd–Se(3)	87.76(9)	Se(4)–C(4)–S(4)	119(1)
Se(1)–Pd–Se(4)	175.6(1)	Se(4)–C(4)–C(5)	124(2)
Se(2)–Pd–Se(3)	174.4(1)	S(4)–C(4)–C(5)	116(2)
Se(2)–Pd–Se(4)	89.92(9)	Se(3)–C(5)–S(5)	121(1)
Se(3)–Pd–Se(4)	91.18(9)	Se(3)–C(5)–C(4)	124(2)
C(1)–S(1)–C(3)	96(1)	S(5)–C(5)–C(4)	115(2)
C(2)–S(2)–C(3)	98(1)	S(4)–C(6)–S(5)	114(1)
C(4)–S(4)–C(6)	97(1)	S(4)–C(6)–S(6)	124(1)
C(5)–S(5)–C(6)	97(1)	S(5)–C(6)–S(6)	122(1)
Se(1)–C(1)–S(1)	119(1)	C(10)–N–C(10 <sup>II</sup> )	109(3)
Se(1)–C(1)–C(2)	122(2)	C(10)–N–C(20)	108(1)
S(1)–C(1)–C(2)	119(2)	C(10)–N–C(20 <sup>II</sup> )	109(1)
Se(2)–C(2)–S(2)	122(1)	C(20)–N–C(20 <sup>II</sup> )	112(3)

Numbers in parentheses are estimated standard deviations (e.s.d.s) in the least significant digits. Symmetry operations: I  $\frac{1}{2} - x, \frac{1}{2} - y, 1 - z$ ; II  $-x, y, \frac{1}{2} - z$ .

**Fig. 6** The unit-cell contents of  $[\text{PMe}_4][\text{Pd}(\text{C}_3\text{S}_3\text{Se}_2)_2]_2$ 

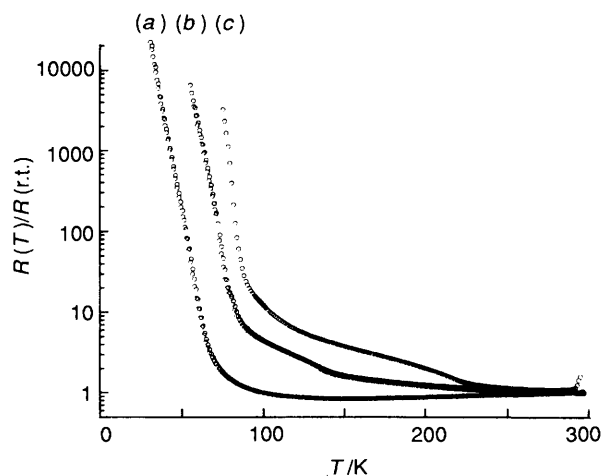
dimers with a Pd–Pd bond length of 3.177 Å, longer than that found in  $\beta$ - $[\text{NMe}_4][\text{Pd}(\text{C}_3\text{S}_5)_2]_2$  (3.116 Å),<sup>3,4</sup> but surprisingly close to that observed in  $[\text{NMe}_4][\text{Pd}(\text{C}_3\text{S}_3\text{Se}_2)_2]_2$  (3.174 Å, see above). The Pd–Pd interaction and S...S repulsions result in an eclipsed overlap of the two Pd(C<sub>3</sub>S<sub>5</sub>)<sub>2</sub> entities within a dimer (Fig. 5), and an out-of-plane displacement of the Pd atom from the S<sub>4</sub> plane (0.07 Å) identical to the corresponding distance (0.07 Å) in  $\beta$ - $[\text{NMe}_4][\text{Pd}(\text{C}_3\text{S}_5)_2]_2$ .<sup>3,4</sup> The structure consists of  $[\{\text{Pd}(\text{C}_3\text{S}_5)_2\}_2]$  dimer layers in the (001) plane separated by sheets of ordered  $\text{PMe}_4$  cations. The dimers are stacked along [110] and  $[\bar{1}\bar{1}0]$ . The Pd(C<sub>3</sub>S<sub>5</sub>)<sub>2</sub> entities are eclipsed within a dimer and slipped between dimers. A number of short (less than sum of the van der Waals radii) intermolecular chalcogen–chalcogen distances are present within the dimers, and between neighbouring stacks, as usually observed in  $M(\text{C}_3\text{S}_5)_2$  compounds,<sup>1</sup> but additional short S...S distances are also observed between stacked dimers (Supplementary material).

**Electrical Properties and Reflectance Spectra of  $[\text{NMe}_4][\text{Pd}(\text{C}_3\text{S}_3\text{Se}_2)_2]_2$ .**—The room-temperature conductivity of this compound is in the range 30–70 S cm<sup>-1</sup>. Fig. 7 shows the temperature dependence of the resistivity. At ambient pressure

**Table 4** Bond lengths (Å) and angles (°) for  $[\text{PMe}_4][\text{Pd}(\text{C}_3\text{S}_5)_2]_2$ 

Pd–Pd <sup>d</sup>	3.1776(9)	S(7)–C(3)	1.748(6)
Pd–S(1)	2.304(1)	S(7)–C(6)	1.730(6)
Pd–S(2)	2.291(3)	S(8)–C(4)	1.729(6)
Pd–S(3)	2.304(1)	S(8)–C(6)	1.717(6)
Pd–S(4)	2.298(2)	S(9)–C(5)	1.644(6)
S(1)–C(1)	1.700(6)	S(10)–C(6)	1.653(6)
S(2)–C(2)	1.684(6)	P–CP(1)	1.787(8)
S(3)–C(3)	1.694(6)	P–CP(1 <sup>II</sup> )	1.787(8)
S(4)–C(4)	1.704(6)	P–CP(2)	1.797(8)
S(5)–C(1)	1.745(5)	P–CP(2 <sup>II</sup> )	1.797(8)
S(5)–C(5)	1.735(6)	C(1)–C(2)	1.381(8)
S(6)–C(2)	1.741(6)	C(3)–C(4)	1.395(8)
S(6)–C(5)	1.716(6)		
Pd <sup>d</sup> –Pd–S(1)	90.25(5)	S(8)–C(6)–S(10)	123.1(4)
Pd <sup>d</sup> –Pd–S(2)	94.56(5)	S(1)–C(1)–S(5)	120.7(3)
Pd <sup>d</sup> –Pd–S(3)	88.97(4)	S(1)–C(1)–C(2)	123.2(4)
Pd <sup>d</sup> –Pd–S(4)	93.54(5)	S(5)–C(1)–C(2)	116.0(4)
S(1)–Pd–S(2)	89.69(5)	S(2)–C(2)–S(6)	121.3(3)
S(1)–Pd–S(3)	90.42(5)	S(2)–C(2)–C(1)	123.4(4)
S(1)–Pd–S(4)	176.17(6)	S(6)–C(2)–C(1)	115.2(4)
S(2)–Pd–S(3)	176.47(6)	S(3)–C(3)–S(7)	121.9(4)
S(2)–Pd–S(4)	89.42(5)	S(3)–C(3)–C(4)	124.2(4)
S(3)–Pd–S(4)	90.23(5)	S(7)–C(3)–C(4)	113.9(4)
C(1)–S(5)–C(5)	97.0(3)	S(4)–C(4)–S(8)	120.9(4)
C(2)–S(6)–C(5)	97.9(3)	S(4)–C(4)–C(3)	122.4(4)
C(3)–S(7)–C(6)	98.2(3)	S(8)–C(4)–C(3)	116.7(4)
C(4)–S(8)–C(6)	97.9(3)	S(5)–C(5)–S(9)	123.8(4)
CP(1)–P–CP(1 <sup>II</sup> )	109.1(6)	S(6)–C(5)–S(9)	122.5(4)
CP(1)–P–CP(2)	108.8(4)	S(7)–C(6)–S(8)	113.3(3)
CP(1)–P–CP(2 <sup>II</sup> )	110.0(4)	S(7)–C(6)–S(10)	123.6(4)
CP(2)–P–CP(2 <sup>II</sup> )	108.1(6)		

Numbers in parentheses are e.s.d.s in the least significant digits. Symmetry operations: I  $\frac{1}{2} - x, \frac{1}{2} - y, -z$ ; II  $-x, y, \frac{1}{2} - z$ .

**Fig. 7** Temperature dependence of the resistance of a sample of  $[\text{NMe}_4][\text{Pd}(\text{C}_3\text{S}_3\text{Se}_2)_2]_2$  (r.t. = room temperature) at 10.7 kbar (a), 5.3 kbar (b) and 1 bar (c)

the resistivity is weakly dependent on the temperature: from room temperature down to 220 K it gradually increases between 220 and 110 K, and finally abruptly increases below 110 K, suggesting some kind of phase transition. The abrupt resistivity increase below 110 K was observed for all three measured samples. However, between 110 and 220 K, the behaviour was sample dependent; one of the samples exhibited metallic behaviour down to 160 K. The conductivity increases when applying pressure: at 10.7 kbar and ambient temperature its value is  $\approx 2.5$  times larger than that determined at ambient pressure. At 10.7 kbar the resistivity remains weakly dependent on the temperature down to  $\approx 70$  K; below this temperature it abruptly increases [ $E_a \approx 0.08$  eV (ca.  $1.28 \times 10^{-20}$  J) at 60 K].

Fig. 8 shows the reflectance spectra recorded at room temperature in the 5000–25 000  $\text{cm}^{-1}$  range. A broad dispersion appears for the polarization parallel to the  $a$  axis. Similar dispersions were observed for several dimerized  $\text{Pd}(\text{C}_3\text{S}_5)_2$  compounds<sup>19</sup> and can be ascribed to the superposition of the two  $\psi_{\text{HOMO}}^+ \rightarrow \psi_{\text{HOMO}}^-$  and  $\psi_{\text{LUMO}}^+ \rightarrow \psi_{\text{LUMO}}^-$  transitions [where  $\psi_{\text{HOMO}}^+$ ,  $\psi_{\text{HOMO}}^-$ ,  $\psi_{\text{LUMO}}^+$  and  $\psi_{\text{LUMO}}^-$  are the energy levels of the bonding and antibonding type of orbitals derived from the highest occupied and lowest unoccupied molecular orbitals of a single  $\text{Pd}(\text{C}_3\text{S}_5)_2$ ]. The appearance of optical excitations of this type in the spectra of  $[\text{NMe}_4][\text{Pd}(\text{C}_3\text{S}_3\text{Se}_2)_2]_2$  strongly suggests an overlap of the energies of the HOMO and LUMO bands due to the presence of dimers along the stacks, and indicates that the conduction band is a HOMO-type band.<sup>21,22</sup>

**Electrical Properties of  $[\text{PMe}_4][\text{Pd}(\text{C}_3\text{S}_5)_2]_2$ .**—The room-temperature conductivity of this compound is  $\approx 20 \text{ S cm}^{-1}$ . Fig. 9 shows the temperature dependence of the resistivity. At ambient pressure the resistivity is weakly dependent from room temperature down to 60 K, and abruptly increases below this temperature. At ambient temperature a linear increase in the conductivity is observed when a quasi-hydrostatic pressure  $P$  is applied. The relative coefficient  $d\sigma/\sigma dP = 0.61 \text{ kbar}^{-1}$  is roughly five to six times higher than for  $\alpha'$ - $[\text{tff}][\text{Pd}(\text{C}_3\text{S}_5)_2]_2$  ( $\text{tff}$  = tetrathiafulvalene cation):<sup>23</sup> this indicates that the crystal lattice of  $[\text{PMe}_4][\text{Pd}(\text{C}_3\text{S}_5)_2]_2$  is less stiff than the lattice of the

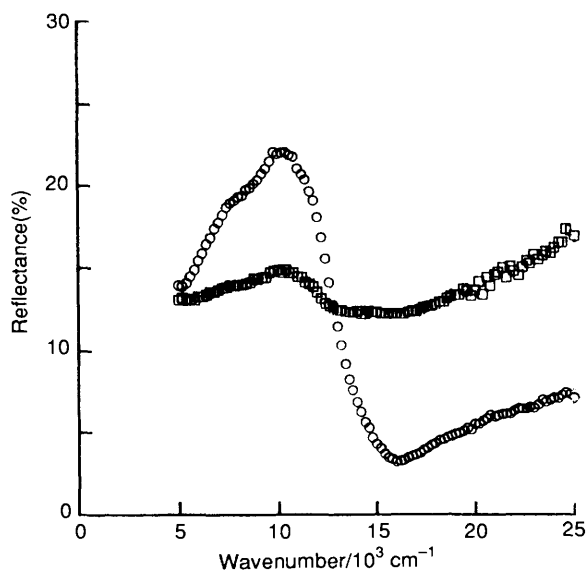


Fig. 8 Reflectance spectra of  $[\text{NMe}_4][\text{Pd}(\text{C}_3\text{S}_3\text{Se}_2)_2]_2$  for polarization parallel to the  $a$  (O) and  $b$  axes (□)

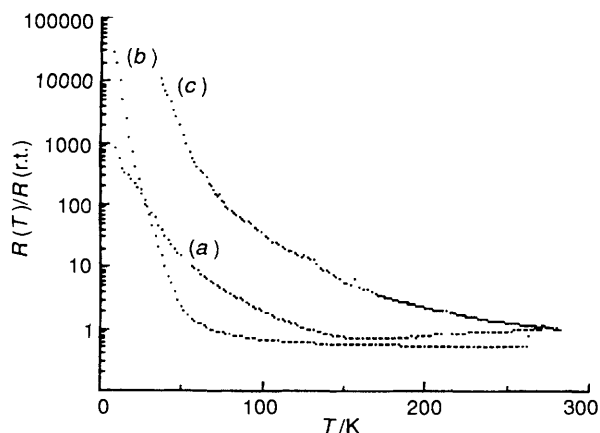


Fig. 9 Temperature dependence of the resistance  $R$  of a sample of  $[\text{PMe}_4][\text{Pd}(\text{C}_3\text{S}_5)_2]_2$  at 15 kbar (a), 10 kbar (b) and 1 bar (c)

tff analogue, whereas the unit-cell volume at ambient pressure and temperature is smaller for  $[\text{PMe}_4][\text{Pd}(\text{C}_3\text{S}_5)_2]_2$  ( $3298 \text{ \AA}^3$ , see above) than for  $\alpha'$ - $[\text{tff}][\text{Pd}(\text{C}_3\text{S}_5)_2]_2$  ( $3394 \text{ \AA}^3$ ).<sup>24</sup> Fig. 9 displays the temperature dependence of the resistance of  $[\text{PMe}_4][\text{Pd}(\text{C}_3\text{S}_5)_2]_2$  at three different pressures. A minimum of the resistivity is observed at 160 K only for the highest pressure, 14.5 kbar. Hence, it is clear that the semiconducting behaviour cannot be suppressed by applying pressure and no sign of superconductivity is found below 15 kbar.

## Conclusion

The  $C2/c$  space group is a common feature observed in most superconducting  $\text{M}(\text{C}_3\text{S}_5)_2$  systems and previous studies on  $\beta$ - $[\text{NMe}_4][\text{Pd}(\text{C}_3\text{S}_5)_2]_2$  indicated that dimerization, often observed in  $\text{Pd}(\text{C}_3\text{S}_5)_2$  systems, does not prevent such systems from being superconducting. Both these observations prompted us to study the closely related  $[\text{NMe}_4][\text{Pd}(\text{C}_3\text{S}_3\text{Se}_2)_2]_2$  and  $[\text{PMe}_4][\text{Pd}(\text{C}_3\text{S}_5)_2]_2$  compounds. These attempts were in a first step successful for in both compounds the  $C2/c$  space group is retained. However, both compounds, in the present state of the art (crystal quality, pressure), do not undergo a superconductive transition. Therefore, only very subtle variations in the structure (unit-cell volume, stacking mode, dimerization mode, etc.) of both {as well of the previously studied  $[\text{AsMe}_4][\text{Pd}(\text{C}_3\text{S}_5)_2]_2$  and  $\text{Cs}[\text{Pd}(\text{C}_3\text{S}_5)_2]_2$ } could explain this difference. Maybe the answer will be found in compared band-structure calculations which will shortly be performed.

## Acknowledgements

This work was in part sponsored by a Centre National de la Recherche Scientifique–Agence Internationale pour la Science et la Technologie (CNRS–AIST) Cooperation Program. We thank D. Maud and J.-C. Portal for use in the study of  $[\text{PMe}_4][\text{Pd}(\text{C}_3\text{S}_5)_2]_2$  of the low-temperature and high-pressure facilities at the Service National des Champs Intenses du CNRS in Grenoble. We also thank J. Reedijk and J. G. Haasnoot for their interest in this work and fruitful discussions about it.

## References

- P. Cassoux, L. Valade, H. Kobayashi, A. Kobayashi, R. A. Clark and A. E. Underhill, *Coord. Chem. Rev.*, 1991, **110**, 115.
- P. Cassoux and L. Valade, in *Inorganic Materials*, eds. D. W. Bruce and D. O'Hare, Wiley, New York, 1991, p. 1.
- A. Kobayashi, H. Kim, Y. Sasaki, R. Kato, H. Kobayashi, S. Moriyama, Y. Nishio, K. Kajita and W. Sasaki, *Chem. Lett.*, 1987, 1819; K. Kajita, Y. Nishio, S. Moriyama, R. Kato, H. Kobayashi, W. Sasaki, A. Kobayashi, H. Kim and Y. Sasaki, *Solid State Commun.*, 1988, **65**, 361.
- A. Kobayashi, H. Kim, Y. Sasaki, K. Murata, R. Kato and H. Kobayashi, *J. Chem. Soc., Faraday Trans.*, 1990, 361; A. Kobayashi, H. Kobayashi, A. Miyamoto, R. Kato, R. A. Clark and A. E. Underhill, *Chem. Lett.*, 1991, 2163; A. Kobayashi and H. Kobayashi, *Kinken Workshop Rep.*, 1992, **11–13**, 90.
- H. Kobayashi, K. Bun, T. Naito, R. Kato and A. Kobayashi, *Chem. Lett.*, 1992, 1909.
- H. Tajima, M. Inokuchi, A. Konayashi, T. Ohta, R. Kato, H. Kobayashi and H. Kuroda, *Chem. Lett.*, 1993, 1235.
- L. Brossard, M. Ribault, L. Valade and P. Cassoux, *Phys. Rev. B.*, 1990, **42**, 3935.
- S. Ravy, J.-P. Pouget, L. Valade and J.-P. Legros, *Europhys. Lett.*, 1989, **9**, 391; S. Ravy, E. Canadell and J.-P. Pouget, in *The Physics and Chemistry of Organic Superconductors*, eds. G. Saito and S. Kagoshima, Springer Proceedings in Physics, Springer, Berlin, 1990, vol. 51, p. 252.
- L. Brossard, M. Ribault, L. Valade and P. Cassoux, *C.R. Acad. Sci., Ser 2*, 1989, **309**, 1117.
- E. Canadell, S. Ravy, J.-P. Pouget and L. Brossard, *Solid State Commun.*, 1990, **75**, 633.
- R. Kato, T. Mori, A. Kobayashi, Y. Sasaki and H. Kobayashi, *Chem. Lett.*, 1984, 1.
- C. Faulmann, J.-P. Legros, P. Cassoux, J. P. Cornelissen, J. G. Haasnoot and J. Reedijk, *Synth. Met.*, 1993, **56/1**, 2063.

- 13 J. P. Cornelissen, C. Faulmann, J.-P. Legros, P. Cassoux, J. G. Haasnoot, P. J. Nigrey and J. Reedijk, *Inorg. Chim. Acta*, 1992, **202**, 131.
- 14 R. Kirmse, J. Stach, W. Dietzsch, G. Steimecke and E. Hoyer, *Inorg. Chem.*, 1980, **19**, 2679.
- 15 R. A. Clark, A. E. Underhill, R. Friend, M. Allen, I. Marsden, A. Kobayashi and H. Kobayashi, in *The Physics and Chemistry of Organic Superconductors*, eds. G. Saito and S. Kagoshima, Springer Proceedings in Physics, Springer, Berlin, 1990, vol. 51, p. 28; A. Izuoka, A. Miyasaki, N. Sato, T. Sugawara and T. Enoki, in *The Physics and Chemistry of Organic Superconductors*, eds. G. Saito and S. Kagoshima, Springer Proceedings in Physics, Springer, Berlin, 1990, vol. 51, p. 32.
- 16 G. M. Sheldrick, SHELX 86, Program for Crystal Structure Solution, University of Göttingen, 1986; C. K. Fair, MolEN, Structure Solution Procedure, Enraf-Nonius, Delft, 1990; D. T. Cromer and J. T. Waber, *International Tables for X-Ray Crystallography*, Kynoch Press, Birmingham, 1974; vol. 4, p. 99, Table 2.2B.
- 17 J. Galy, R. Enjalbert, P. Millet, C. Faulmann and P. Cassoux, *J. Solid State Chem.*, 1988, **74**, 356.
- 18 K. Yakushi, M. Iguchi and H. Kuroda, *Bull. Chem. Soc. Jpn.*, 1979, **52**, 3180.
- 19 R. A. Clark and A. E. Underhill, *Synth. Met.*, 1988, **27**, 515; A. E. Underhill, R. A. Clark, I. Marsden, M. Allen, R. H. Friend, H. Tajima, T. Naito, M. Tamura, H. Kuroda, A. Kobayashi, H. Kobayashi, E. Canadell, S. Ravy and J.-P. Pouget, *J. Phys. (Paris)*, 1991, **C3**, 933.
- 20 J. P. Cornelissen, Ph.D. Thesis, University of Leiden, 1992.
- 21 E. Canadell, E. I. Rachidi, S. Ravy, J.-P. Pouget, L. Brossard and J.-P. Legros, *J. Phys. (Paris)*, 1989, **50**, 2967; S. Ravy, E. Canadell, J.-P. Pouget, P. Cassoux and A. E. Underhill, *Synth. Met.*, 1991, **41-43**, 2191.
- 22 H. Tajima, T. Naito, M. Tamura, A. Kobayashi, H. Kuroda, R. Kato, H. Kobayashi, R. A. Clark and A. E. Underhill, *Solid State Commun.*, 1991, **79**, 337.
- 23 L. Brossard, H. Hurdequint, M. Ribault, L. Valade, J.-P. Legros and P. Cassoux, *Synth. Met.*, 1988, **27**, B157; L. Brossard, M. Ribault, L. Valade and P. Cassoux, *J. Phys. (Paris)*, 1989, **50**, 1521.
- 24 J.-P. Legros and L. Valade, *Solid State Commun.*, 1988, **68**, 599.

Received 23rd July 1993; Paper 3/04368A